The changes observed in the absorption and emission spectra of the drug on addition of liposomes were considerably larger at pH 5.0 than at higher pH investigated (6.0 and 7.4). At pH 5.0, with increasing lipid concentration, first a decrease was observed in the emission intensity of the 660 nm band dominant in the drug emission in neat buffer. At higher lipid concentration, fluorescence intensity increased with the dominant band shifting to ~ 680 nm (fig. L.12.1a). These observations are consistent with the fact that the neutral species of the drug abundant at low pH will bend strongly enough even at low lipid concentration, and suggest that, as a consequence, the amount of drug per liposome increases up to such an extent that self quenching of fluorescence occurs. This effect gets reduced as the pH of the medium is increased, as increased pH produces more anionic species, and since they are less hydrophobic than the neutral ones, the binding with the liposomes becomes less favorable and consequently the self-quenching of fluorescence in the lipid bilayer decreases.

To further confirm these aspects we measured the pH dependence of the fluorescence decay time of the drug for varying lipid concentration. The results in fig. L.12. 1b show that for a given concentration of the drug, at pH 5.0 the fluorescence decay was faster for liposome concentrations where the fluorescence quenching was observed to be significant and was slower at larger liposome concentrations. For higher pH the dependence of the decay times on concentration of liposomes was much smaller. Similarly fluorescence quenching experiments with iodide ions confirmed that while at pH 5.0 the drug bound to liposome is inaccessible to the quencher and hence located deep inside the lipid bilayer, for pH 6.0 and higher where the anionic species are a majority, the drug binds closer to the liposome interface. [For details see: *K. Das, B. Jain, A. Dube and P.K. Gupta, Chemical Physics Letters, Vol. 401, page 185-188, (2005)*].

(Contributed by : P. K. Gupta; pkgupta@cat.ernet.in)

L.13 Laser welding of automobile transmission gear assemblies

Laser welding of automobile transmission gear assemblies has been established. In the first phase of the study, a few gear assembly blanks were laser welded using the indigenously developed high power continuous wave CO_2 laser, and mechanical and metallurgical characterizations were carried out. Good quality weld, up to 4 mm depth, with narrow heat affected zone was produced at 2.5-3 kW laser power and 1mm/min weld speed. Argon gas was used as a shielding gas during laser welding. Mechanical strength of the weld joint confirmed the specifications.

Fig. L.13.1 *Laser welded gear assemblies*

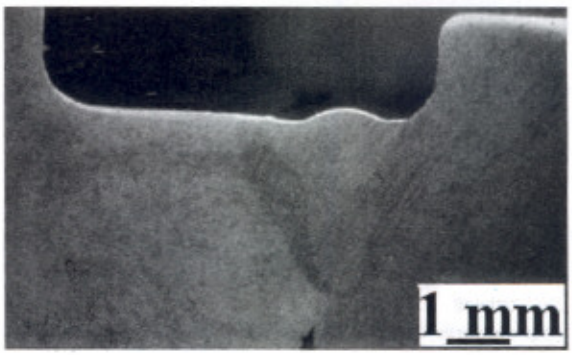

Fig. L.13.2 *Macroscopic view of Laser weldment cross-section*

In the second phase, about 230 numbers of different kinds of automobile transmission gear assemblies were laser welded for functional testing. Fig. L.13.1 presents photographs of laser welded gear assemblies, while fig. L.13.2 show a macroscopic view of the cross-section and close up of one of the laser weldments respectively.

(Contributed by: Harish Kumar; harishk@cat.ernet.in and A.K. Nath)

L.14 Improved mechanical properties of Inconel-625 components by laser rapid manufacturing

Laser rapid manufacturing (LRM) is an upcoming rapid manufacturing technology, being developed at the various laboratories around the world. It is similar to laser cladding at process level with different end applications. In general, laser cladding technique is used to deposit material on the substrate, either to improve the surface properties or to refurbish the worn out parts, while LRM is capable of near net shaping the components by layer-by-layer deposition of the material directly from CAD model.

Inconel-625 is a nonmagnetic, corrosion- and oxidation-resistant, nickel-based alloy, which is used widely in heat shields, furnace hardware, gas turbine engine ducting, combustion liners and spray bars, chemical plant hardware and special seawater applications. Using indigenously developed LRM facility, the LRM process for the Inconel-625 component fabrication has been established. The tensile and impact resistance properties of the LRM material have been evaluated for various directions of deposition. LRM fabricated machined tensile test specimen are shown in fig. L.14.1

Fig. L.14.1 *LRM fabricated machined tensile specimen*

The results of tensile testing are summarized in Table L.14.1. It is found that LRM material has superior tensile strength without sacrificing percentage elongation as compared to that of wrought material, while the impact resistance of the material is at par with that of conventionally processed material.

The microstructure examinations revealed that there were finely intermixed dendritic and cellular microstructures with high dislocation density. Fig. L.14.2 presents the microstructure of LRM fabricated Inconel-625 specimen.

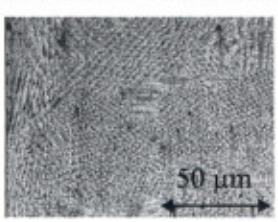

Fig. L.14.2 *Microstructure of LRM fabricated Inconel-625 specimen*

The direction of dendrite growth was along the direction of deposition. The fine dendrite formation was due to inherent rapid cooling rate during LRM, while cellular microstructure is attributed to relatively reduced cooling rate during multi-layer deposition. The fine dendritic formation with high dislocation density are responsible for higher mechanical strength, while formation of cellular microstructure has helped in keeping ductility intact. Using the established process parameters, several components like-impeller, cage, multi-layer walls etc. have been successfully fabricated.

(Contributed by: C P Paul; paulcp@cat.ernet.in,
P. Ganesh and A.K. Nath)

L.15 Efficient 60 W green beam generation by use of an intracavity frequency-doubled diode side-pumped Q switched Nd:YAG rod laser

We have achieved 60 W of average green power by using copper coated pump beam reflector and 80 ^{0}C phase-matched KTP crystal. The schematic of the laser set up is shown in fig. L.15.1. The laser set up consists of a pump head, a resonator, an acousto-optic Q-switch and a KTP crystal for intracavity frequency doubling. The pump head consists of a 0.6 at.% doped 100 mm long (4 mm diameter) Nd:YAG crystal placed within a copper-coated flow tube. Nine numbers of 1cm laser diode bars were grouped in 3-fold symmetry for transverse pumping of the rod.

The cavity was V-shaped in order to provide proper spot sizes at the rod and at the KTP crystal. The rear flat mirror (M1) was highly reflecting (R> 99.7%) at the fundamental wavelength. The flat end mirror (M3) is highly reflecting (R> 99.7%) at the fundamental wavelength as well as at the second harmonic wavelength at 532 nm in order to retro-reflect the green beam generated in the backward direction. The folding mirror M2 was a concave mirror with 200 mm radius of curvature and was coated for high reflection at the fundamental wavelength and high transmission at the second harmonic wavelength in order to provide a means to couple

Table L.14.1 Tensile and impact properties of differently processed Inconel-625

Material	Direction of deposition	0.2% yield stress	Ultimate tensile stress	Elongation	Impact resistance
LRM fabricated	0°	572±25 MPa	920±15 MPa	48±2 %	104±2 J
	90°	568±20 MPa	925±12 MPa	46±2 %	102±1 J
	Mixed	571±15 MPa	915±20 MPa	49±3 %	103±1 J
Hot finished & annealed	-	395±15 MPa	824±25 MPa	51±4 %	110±5 J